Available online at www.sciencedirect.com

ScienceDirect

www.elsevier.com/locate/jes

JES JOURNAL OF ENVIRONMENTAL SCIENCES

www.jesc.ac.cn

Methyl Orange removal by a novel PEI-AuNPs-hemin nanocomposite

*Weiwen Hu[1,**], Xuehua Yu[1,**], Qiong Hu[1], Jinming Kong[1,*], Lianzhi Li[2], Xueji Zhang[3,*]*

1. *School of Environmental and Biological Engineering, Nanjing University of Science & Technology, Nanjing 210094, China.*
E-mail: weiwen_hu@163.com
2. *Shandong Provincial Key Laboratory of Chemical Energy Storage and Novel Cell Technology, School of Chemistry and Chemical Engineering, Liaocheng University, Liaocheng 252000, China*
3. *Chemistry Department, College of Arts and Sciences, University of South Florida, FL 33620-4202, USA*

ARTICLE INFO

Article history:
Received 12 August 2015
Revised 2 January 2016
Accepted 4 January 2016
Available online 4 March 2016

Keywords:
Poly(ethyleneimine)
Hemin
Au nanoparticle
Nanocomposite
Methyl Orange removal

ABSTRACT

A novel poly(ethyleneimine)/Au nanoparticles/hemin nanocomposite (PEI-AuNPs-Hemin) acting for Methyl Orange (MO) removal has been synthesized. PEI-AuNPs was prepared firstly and it was then linked to hemin through the coupling between carboxyl groups in hemin and amino groups in PEI without the activation of carboxyl groups. The high reactivity and stability of AuNPs contributed greatly in the formation of the amido bonds in the nanocomposite. Fourier transform infrared spectroscopy, transmission electron microscopy and UV–visible spectroscopy were used to characterize the PEI-AuNPs-Hemin. Results show that PEI-AuNPs-Hemin has strong adsorption for MO. Adsorption and degradation experiments were carried out at different pHs, nanocomposite concentrations and UV irradiation times. Removal of MO in acidic solutions was more effective than in basic solutions. The real-time study showed that the MO degradation with the nanocomposite under UV irradiation was a fast process. In addition, the photocatalytic degradation mechanism was proposed. The study suggests that the PEI-AuNPs-Hemin may have promising applications in environmental monitoring and protection.

Introduction

Synthetic dyes are commonly used in industries, such as food, medicine, paper, textile and cosmetics. Most of them are toxic, carcinogenic, and mutagenic for human body. Each year a large amount of dyes in untreated wastewater are discharged into the ecological systems, resulting in adverse effects on human and animal health. Therefore, they must be carefully removed from the environment (Goscianska et al., 2014; Zhang et al., 2014). Some new chemical and biological methods for dye removal have been reported, such as oxidation (Meriç et al., 2004), electrolysis (Cui et al., 2012), membrane separation (Zhong et al., 2012), coagulation and flocculation (Verma et al., 2012). However, due to the complex molecular structures and high stability of dyes, these methods are not always successful. Development of nanocomposites for dye removal has increased tremendously, such as multi-walled carbon nanotube functionalized with chitosan and poly-2-hydroxyethyl methacrylate for Methyl Orange (MO) removal (Mahmoodian et al., 2015), γ-Fe_2O_3 nanoparticles integrated $H_2Ti_3O_7$ nanotubes for Methylene Blue removal (Harsha et al., 2015), reduced grapheme oxide enwrapped AgI nanocomposites for Rhodamine B removal (Reddy et al., 2015), magnetic nickel zinc ferrite nanocomposite for organic synthesized dyes removal (Afkhami et al., 2015), *etc.*

* *Corresponding authors.*
** *These authors contributed equally.* E-mail: j.kong@njust.edu.cn (Jinming Kong), xueji@usf.edu (Xueji Zhang).

http://dx.doi.org/10.1016/j.jes.2016.01.016
1001-0742/

Nanocomposites have the advantages of large specific surface area, small diffusion resistance, high adsorption capacity and faster adsorption equilibrium (Ahmad et al., 2015).

Hemin, a biologically active iron-porphyrin compound, is considered a potential biomimetic catalyst for water purification (Xue et al., 2012). However, despite the prominent properties of hemin, difficulties remain in the direct application of hemin as a catalyst in aqueous solution due to its oxidative self-destruction in the oxidizing reaction system, and molecular aggregation which results in catalytically inactive dimers (Yao et al., 2014). Thus there is a growing demand for overcoming these problems. One potential method is to immobilize hemin on various supports, such as TiO_2 (Tang et al., 2013), β-cyclodextrin (Lin et al., 2012) or graphene (Guo et al., 2011) to improve reactivity and stability in oxidation reactions. However, TiO_2-hemin showed weak reactivity, and β-cyclodextrin-hemin or grapheme-hemin was difficult to separate from the reaction system. Consequently, the development of novel materials as supports to immobilize hemin for dye removal with improved reactivity, stability, dispersion, separability and easy synthesis is highly desired.

In the past few decades, a variety of nanomaterials have been developed for immobilization and stabilization of biomolecules (Ansari and Husain, 2012). Among these exploited nanomaterials, gold nanoparticles (AuNPs) are highly attractive because of their unique properties including high stability and reactivity, biocompatibility, excellent electronic conductivity and surface plasma characteristic (Jans and Huo, 2012; Saha et al., 2012). AuNPs have been successfully applied for the immobilization of biomolecules such as DNA (Pei et al., 2012), enzyme (He et al., 2011), antibody (Stuchinskaya et al., 2011) and polymer (Coulston et al., 2011). Polyethyleneimine (PEI) is a typical water-soluble and mono-disperse polyamine with regular branched dimensional structure. There are a large number of nitrogen atoms in its macromolecular chain. It has been widely used for modification, catalysis and reduction (Kim et al., 2008; Liu et al., 2013). Wang et al. (2005) reported that the secondary amino groups of the PEI as linear units are related to the reduction process, and the primary amino groups as terminal units are responsible for the particle stabilization. Brondani et al. (2013) have successfully applied PEI-coated AuNPs (PEI-AuNPs) for laccase immobilization. Given that AuNPs can also serve as photocatalysts for dye degradation under UV irradiation (Cheng et al., 2013; Zhu et al., 2009), we synthesized PEI-AuNPs using PEI as a reductant and stabilizer to immobilize the hemin through the formation of amido bonds.

In this work, a novel PEI-AuNPs-Hemin nanocomposite applied for MO removal has been successfully synthesized. The nanocomposite was easily dispersed and stable in aqueous solutions, and exhibited strong adsorption for MO. MO removal experiments were carried out at different pH, nanocomposite concentrations and UV irradiation times. Compared with other nanocomposites reported before (Afkhami et al., 2015; Harsha et al., 2015; Mahmoodian et al., 2015; Reddy et al., 2015), PEI-AuNPs-Hemin is easier to synthesize and more effective (degrading 80% MO within 2 min with only 0.5 mg/mL PEI-AuNPs-Hemin), which make it potentially applied in environmental monitoring and protection.

1. Experimental

1.1. Chemicals

Branched PEI (weight-average molecular weight, 25 kDa), $HAuCl_4 \cdot 4H_2O$ and Hemin (99%) were purchased from Sigma-Aldrich (St. Louis, MO, USA). N,N-dimethylformamide (DMF) was obtained from Sinopharm Chemical Reagent Co., Ltd. (Shanghai, China). All reagents used were of analytical grade. Ultrapure water was prepared through a Millipore Milli-Q water purification system (≥18.25 MΩ).

1.2. Instruments

UV–visible absorbance spectra were measured on an UV-3600 UV–VIS-NIR spectrophotometer (Shimadzu, Japan) with a sample volume of 3 mL. Infrared spectra were carried out on Fourier transform infrared spectroscopy (FTIR-8400S, Shimadzu, Japan). Transmission electron microscopy (TEM) measurements were performed on a HITACHI H-8100 EM transmission electron microscope (Hitachi, Japan). TEM samples were prepared by spin coating 10 μL of the mixture onto carbon-coated copper grid substrates, which were then baked at 70°C.

1.3. Preparation of PEI-AuNPs-hemin

The AuNPs were synthesized following the procedure described by Brondani et al.2013). Firstly, 500 μL of PEI solution was added to 5 mL of 1 mmol/L $HAuCl_4$ solution with stirring. The mixture was then heated to 80°C with a ramping of 5°C/min and held at 80°C until the characteristic ruby red color appeared (generally 2 min). The PEI-AuNPs nanocomposite was obtained after cooling down to the ambient temperature under stirring. Then, 1 mL PEI-AuNPs solution was mixed with 500 μL of 0.1 mmol/L hemin. After stirring for 1 hr, the mixture was centrifuged at 14,000 r/min for 30 min, then washed and

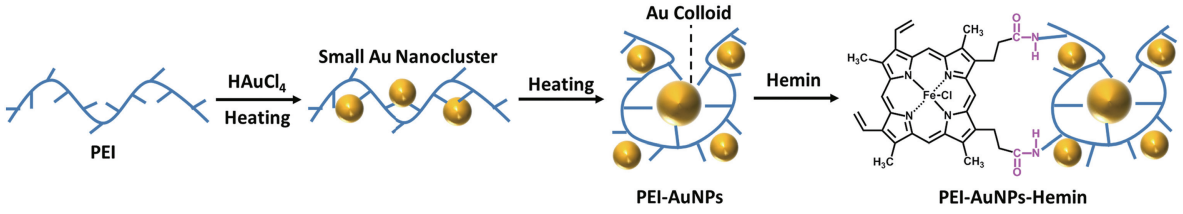

Fig. 1 – Schematic representation for the formation of poly(ethyleneimine)/Au nanoparticles/hemin nanocomposite (PEI-AuNPs-Hemin).

centrifuged again in deionized water for further 20 min. PEI-AuNPs were linked to hemin through the coupling between carboxyl groups in hemin and amino groups in PEI without the activation of carboxyl groups. The high reactivity and stability of AuNPs contributed greatly in the rapid formation of the stable amido bonds in PEI-AuNPs-Hemin nanocomposite. The nanocomposite was synthesized successfully according to the FT-IR and TEM characterization. Samples for MO removal were prepared by diluting the nanocomposite in deionized water with a final concentration of 0.5 mg/mL. The procedures for the synthesis of PEI-AuNPs-Hemin nanocomposites are illustrated in Fig. 1.

1.4. Dye removal

Various volumes of 0.5 mg/mL PEI-AuNPs-Hemin were added to 3 mL of 25 μmol/L MO solutions, respectively. The absorbance of the mixture was recorded on an UV-3600 UV–VIS-NIR spectrophotometer (Shimadzu, Japan) with a sample volume of 3 mL.

2. Results and discussion

2.1. Characterization of materials

To synthesize PEI-AuNPs-Hemin nanocomposite, PEI-AuNPs were firstly prepared. When PEI was mixed with $HAuCl_4$, ion pairs were formed between protonated amine cations of PEI and $AuCl_4^-$ anions. Then instable double bounds were generated. With the continuous heating, Au^0 atoms were formed from the $AuCl_4^-$ precursor and amide bounds were generated. These Au^0 atoms could collide with each other to form small nanoclusters. When some AuNPs were fully coated with PEI, which prevented the immobilization of another PEI molecule due to the electrostatic repulsion, uncoupled colloids were formed. On the other hand, when some AuNPs were partially coated with PEI, the polyamine acted as a linker bridging different particles into aggregates (Köth et al., 2008; Wang et al., 2005).

The as-synthesized PEI-AuNPs-Hemin nanocomposite was characterized by FT-IR and TEM. The samples for FT-IR were prepared by dispersing the nanocomposite in methanol. As can be seen from Fig. 2a, the band at 3441 cm^{-1} is attributed to the stretching vibration of N-H from PEI. The peak at 1655 cm^{-1} is the characteristic peak of amido bond owing to the stretching vibration of C═O, which reveals that the secondary amido bond exists in the nanocomposite. The peak at 1489 cm^{-1} is ascribed to the N–H in-plane vibration and the peak at 687 cm^{-1} is due to the out-of-plane bending vibration of $–CH_3$ from the aromatic pyrrole ring of hemin. From the FT-IR spectrum, we can conclude that hemin and PEI-AuNPs in the nanocomposite were connected through amido bonds. The high reactivity and stability of AuNPs contributed greatly in the formation of the amido bonds (Wang et al., 2011). As shown in Fig. 2b, the PEI-AuNPs-Hemin nanocomposite presented an average diameter of 10.5 ± 1.5 nm. The TEM image revealed that the nanocomposite had a spherical morphology approximately.

2.2. Adsorption property of PEI-AuNPs-hemin

The adsorption ability of PEI-AuNPs-Hemin for MO as a model pollutant was investigated. Fig. 3 shows the experimental results for the adsorption of 25 μmol/L MO on PEI-AuNPs-Hemin. An obvious UV–vis absorbance centered at 501 nm was clearly observed. When adding 10 μL of 0.1 mmol/L hemin solution to 3 mL of MO, the absorbance of MO was hardly changed. The absorbance was still nearly unchanged after further addition of 10 μL hemin. Then we tried to investigate the adsorption of MO in PEI-AuNPs solution. Results showed that the absorbance of MO was also nearly unchanged, indicating that PEI-AuNPs had no adsorption toward MO. However, a dramatic drop of absorbance was observed (yellow curve in Fig. 3) when merely 10 μL of PEI-AuNPs-Hemin was added to the dye solution (the final concentration of PEI-AuNPs-Hemin was 1.7 mg/L). As reported before (Dai et al., 2007), the peak at about 395 nm may be attributed to an intermediate formed by demethylation, methylation or hydroxylation process or their combination. It might originate from the interaction between the transient fragment species after breaking down the azo group. The intermediate has short retention time of several minutes. The results illustrated that the nanocomposite had strong adsorption toward MO. It should be pointed out that, in addition to the intrinsic nature, the relatively high surface area and nano-structure of PEI-AuNPs-Hemin had also contributed to the good adsorption capacity.

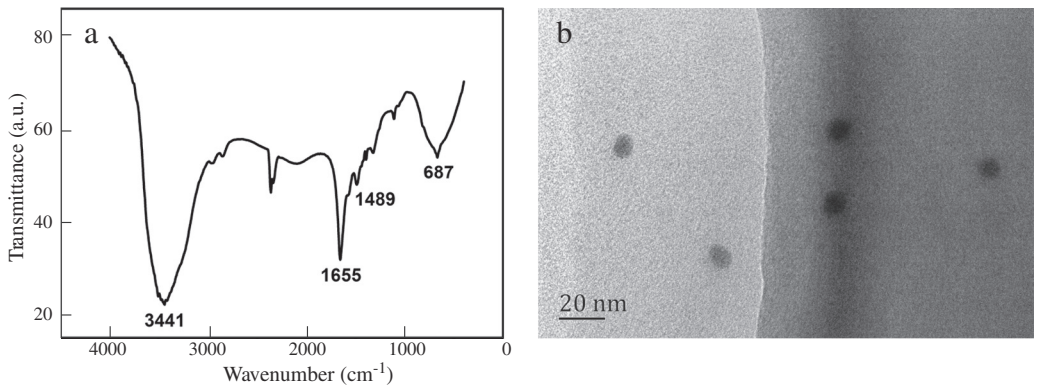

Fig. 2 – (a) Fourier transform infrared (FT-IR) spectra of the PEI-AuNPs-Hemin nanocomposite; (b) transmission electron microscopy (TEM) image of the PEI-AuNPs-Hemin nanocomposite.

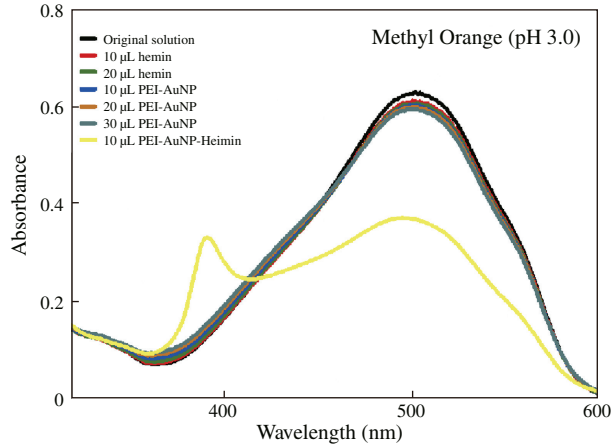

Fig. 3 – The effect of hemin, PEI-AuNPs and PEI-AuNPs-Hemin on the absorbance of Methyl Orange (MO) (pH 3.0).

To obtain the optimal adsorption capacity of the nanocomposite, relationship between adsorbent dosage and dye removal was studied by varying the adsorbent quantity while keeping the initial dye concentration unchanged. As indicated in Fig. 4, the characteristic absorbance of 25 μmol/L MO at 501 nm decreased upon increasing the concentration of PEI-AuNPs-Hemin. The MO adsorption capacity of PEI-AuNPs-Hemin enhanced accordingly as the nanocomposite concentration increasing and eventually reached saturation, which was highly remarkable compared with PEI-AuNPs. The observed increasing of the adsorption capacity may be attributed to: (1) the increase in the degree of dye molecules absorbed on the catalyst surface; (2) the increase in the number of surface active sites; and (3) the increase in the surface area.

pH is an important parameter for an adsorption reaction, and it is related to several factors including (1) charges on the nanocomposite surface; (2) nature of the dye (cationic/anionic/neutral); (3) magnitude of the adsorption on nanocomposites surface. Fig. 5 shows adsorption kinetic curve of MO at different concentrations of PEI-AuNPs-Hemin in a series of pH. It can be seen that the MO adsorption on PEI-AuNPs-Hemin was dramatically influenced by pH. The adsorption and the final removal efficiency increased with pH decreasing and the MO adsorption was highly effective at pH 3.0. When only 10 μL of PEI-AuNPs-Hemin was added into the 3 mL of 25 μmol/L MO (the final concentration of PEI-AuNPs-Hemin was 1.7 mg/L), the absorbance of MO decreased by 36.5%. The absorbance of MO decreased steadily with further addition of PEI-AuNPs-Hemin and reached almost zero when the added amount increased to 120 μL (the final concentration of PEI-AuNPs-Hemin was 19.2 mg/L). The amount of PEI-AuNPs-Hemin required for removing the same amount of MO decreased with the pH increasing. At pH 10, the nanocomposite almost had no effect on the MO adsorption.

The lower pH in aqueous solution may help to reactivate the Fe^{3+} contained in hemin, thus enhancing the degradation reaction on the surface of PEI-AuNPs-Hemin nanocomposite. On the other hand, at acidic condition, MO formed a quinoid structure through protonation, resulting in decreased bond energy. MO was easily oxidized by the generated electron hole on PEI-AuNPs-Hemin, so acidic condition favored the degradation of MO. At pH ≥ 7, MO existed as an anion in aqueous solution. The dissociation of the sodium ion and the electrostatic repulsion between the anionic MO molecules and nanocomposite in alkaline condition could not enhance their collision to achieve an effective degradation of MO (Lien et al., 2006). Hence, we chose pH 3.0 as the optimal condition for the MO removal with PEI-AuNPs-Hemin.

2.3. Photocatalytic degradation studies of PEI-AuNPs-Hemin

In addition to the intrinsic peroxidase-like catalytic activity, PEI-AuNPs-Hemin also exhibited a strong ability to degrade MO with short-time UV exposure at pH 3.0. Under acidic conditions, dominant photoactive species were produced, resulting in high yield of hydroxyl radicals along with regeneration of numerous Fe^{2+} ions (Benkelberg and Warneek, 1995). This could induce efficient dye degradation. To investigate the potential application of PEI-AuNPs-Hemin as a photocatalyst, we used the

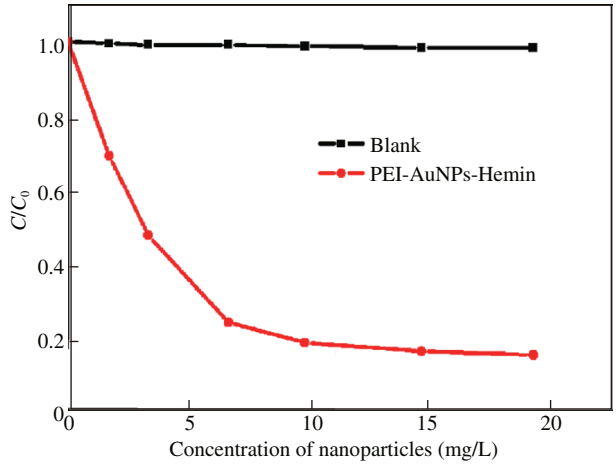

Fig. 4 – The MO adsorption with the PEI-AuNPs-Hemin and PEI-AuNPs of different concentrations (pH 3.0).

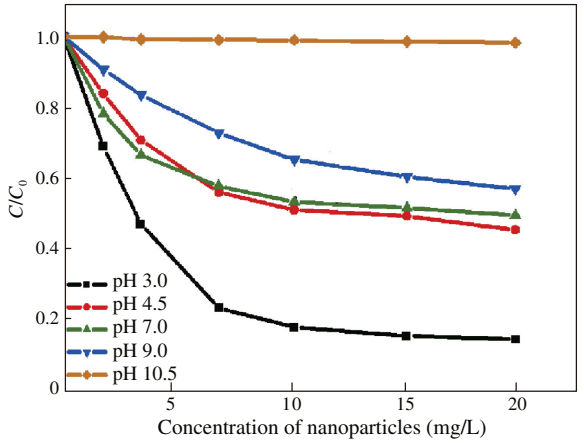

Fig. 5 – The kinetic adsorption data of MO versus different concentration of PEI-AuNPs-Hemin at different pH.

nanocomposite for MO degradation under 280 nm UV irradiation. The extents of MO degradation versus irradiation time for various systems were investigated. As seen in Fig. 6, in the presence of PEI-AuNPs-Hemin, the degradation of MO proceeded much more rapidly than those without it. Over 80% of MO was decomposed in the first 2 min, indicating that PEI-AuNPs-Hemin had ultrafast degradation kinetics toward dye solutions. This enhancement in photocatalytic activity of PEI-AuNPs-Hemin system was attributed to the reduction of electron hole recombination speeds. Upon UV irradiation, charge carriers were generated as shown in Eq. (1).

$$\text{PEI-AuNPs-Hemin}\left(Fe^{3+}\right) + h\nu \rightarrow \text{PEI-AuNPs}^{(e^- + H^+)}\text{-Hemin}\left(Fe^{3+}\right) \quad \text{Electron trapped by PEI-AuNPs} \tag{1}$$

$$\text{PEI-AuNPs}^{(e^- + H^+)}\text{-Hemin}\left(Fe^{3+}\right) \rightarrow \text{PEI-AuNPs-Hemin}\left(Fe^{2+}\right) \quad \text{Electron trapped by hemin} \tag{2}$$

The photogenerated electrons in the conduction band (CB) of PEI-AuNPs-Hemin were transferred in two different pathways: (1) the CB electron are immediately transferred to Fe^{3+} ion present in the hemin molecule, reducing the ferric hemin to ferrous hemin as shown in Eq. (2); (2) the CB electrons are transferred to molecular oxygen, reducing it to superoxide anion radical $O_2^{\bullet -}$ as shown in Eqs. (3) and (4).

$$\text{PEI-AuNPs}^{(e^-)}\text{-Hemin}\left(Fe^{3+}\right) + O_2 \rightarrow O_2^{\bullet -} \quad \text{Electron trapped by } O_2 \tag{3}$$

$$\text{PEI-AuNPs-Hemin}\left(Fe^{2+}\right) + O_2 \rightarrow O_2^{\bullet -} + \text{PEI-AuNPs-Hemin}\left(Fe^{3+}\right) \quad \text{Electron trapped by hemin} \tag{4}$$

According to the crystal field theory, the reduced ferrous hemin (Fe^{2+}) is relatively unstable due to the loss of d^5 electronic configuration and tends to return immediately to $Fe^{3+}(d^5)$ state to attain stable electronic configuration. Consequently, Fe^{2+} could be oxidized to Fe^{3+} by transferring electron for O_2 molecule adsorption on PEI-AuNPs-Hemin. Shallow trapping of photo-generated electron by ferric ion of hemin (Fe^{3+}) and de-trapping of this electron to attain stable half-filled electronic configuration was a continuous cyclic process. Similar mechanism had been proposed for molecular compounds on TiO_2 complex interfaces (Devi and Arunakumari, 2013; Obare et al., 2003). The photo-generated holes could oxidize the dye molecules by producing hydroxyl radicals, which act as powerful oxidants as shown in Eq. (5), $O^{2\bullet -}$ and $OH^{\bullet}$ were also capable of oxidatively degrading the dye (Eq. (6)).

$$h^+ + OH_{(surf)}{}^- \rightarrow OH_{(surf)}{}^{\bullet} \tag{5}$$

$$OH_{(surf)}{}^{\bullet} + MO \rightarrow CO_2 + H_2O \tag{6}$$

The analysis suggests that PEI-AuNPs-Hemin was an effective photocatalyst for degradation of MO in water under UV irradiation.

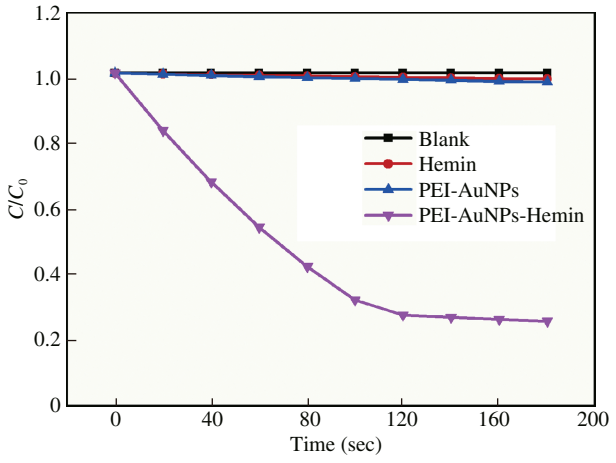

Fig. 6 – The kinetic degradation data of MO versus UV irradiation time in different systems, ultrapure water; 0.1 mmol/L hemin; 0.5 mg/mL PEI-AuNPs; 0.5 mg/mL PEI-AuNPs-Hemin (pH 3.0).

3. Conclusions

In summary, we demonstrated a novel and facile strategy to prepare PEI-AuNPs-Hemin nanocomposite for Methyl Orange removal. The formation of amido bonds linking PEI and hemin in the nanocomposite has not been reported. The synthesis was greatly attributed to the high reactivity and stability of AuNPs. Benefiting from the combined advantages of PEI-AuNPs and hemin, the novel nanocomposite showed effective and enhanced adsorbability for removal of dye (MO) in acidic solutions. In addition, degradation of MO took place immediately upon UV irradiation, indicating that PEI-AuNPs-Hemin could act as a photocatalyst. The excellent photocatalytic property of PEI-AuNPs-Hemin was further discussed in relation to its microstructure. This study suggests that PEI-AuNPs-Hemin may have promising applications in environmental monitoring and protection.

Acknowledgments

This work was supported by the National Natural Science Foundation of China (No. 21575066) and the Technology Foundation for Selected Overseas Scholar in Nanjing.

REFERENCES

Afkhami, A., Sayari, S., Moosavi, R., Madrakian, T., 2015. Magnetic nickel zinc ferrite nanocomposite as an efficient adsorbent for the removal of organic dyes from aqueous solutions. J. Ind. Eng. Chem. 21, 920–924.

Ahmad, A., Mohd-Setapar, S.H., Chuong, C.S., Khatoon, A., Wani, W.A., Kumar, R., Rafatullah, M., 2015. Recent advances in new generation dye removal technologies: Novel search for approaches to reprocess wastewater. RSC Adv. 5, 30801–30818.

Ansari, S.A., Husain, Q., 2012. Potential applications of enzymes immobilized on/in nano materials: A review. Biotechnol. Adv. 30, 512–523.

Benkelberg, H.J., Warneek, P., 1995. Photodecomposition of iron (III) hydroxo and sulfato complexes in aqueous solution: Wavelength dependence of OH and SO^{4-} quantum yields. J. Phys. Chem. 34, 5214–5221.

Brondani, D., de Souza, B., Souza, B.S., Neves, A., Vieira, I.C., 2013. PEI-coated gold nanoparticles decorated with laccase: A new platform for direct electrochemistry of enzymes and biosensingapplications. Biosens. Bioelectron. 42, 242–247.

Cheng, N., Tian, J., Liu, Q., Ge, C., Qusti, A.H., Asiri, A.M., Al-Youbi, A.O., Sun, X., 2013. Au-nanoparticle-loaded graphitic carbon nitride nanosheets: Green photocatalytic synthesis and application toward the degradation of organic pollutants. ACS Appl. Mater. Interfaces 5, 6815–6819.

Coulston, R.J., Jones, S.T., Lee, T.C., Appel, E.A., Scherman, O.A., 2011. Scherman, supramolecular gold nanoparticle-polymer composites formed in water with cucurbit [8] uril. Chem. Commun. 47, 164–166.

Cui, D., Guo, Y.Q., Cheng, H.Y., Liang, B., Kong, F.Y., Lee, H.S., Wang, A.J., 2012. Azo dye removal in a membrane-free up-flow biocatalyzed electrolysis reactor coupled with an aerobic bio-contact oxidation reactor. J. Hazard. Mater. 239, 257–264.

Dai, K., Chen, H., Peng, T., Ke, D., Yi, H., 2007. Photocatalytic degradation of methyl orange in aqueous suspension of mesoporous titania nanoparticles. Chemosphere 69, 1361–1367.

Devi, L.G., Arunakumari, M.L., 2013. Enhanced photocatalytic performance of Hemin (chloro (protoporhyinato) iron (III)) anchored TiO_2 photocatalyst for methyl Orange degradation: A surface modification method. Appl. Surf. Sci. 276, 521–528.

Goscianska, J., Marciniak, M., Pietrzak, R., 2014. Mesoporous carbons modified with lanthanum (III) chloride for methyl orange adsorption. Chem. Eng. J. 247, 258–264.

Guo, Y., Deng, L., Li, J., Guo, S., Wang, E., Dong, S., 2011. Hemin-graphene hybrid nanosheets with intrinsic peroxidase-like activity for label-free colorimetric detection of single-nucleotide polymorphism. ACS Nano 5, 1282–1290.

Harsha, N., Krishna, K.S., Renuka, N.K., Shukla, S., 2015. Facile synthesis of γ-Fe_2O_3 nanoparticles integrated $H_2Ti_3O_7$ nanotubes structure as a magnetically recyclable dye-removal catalyst. RSC Adv. 5, 30354–30362.

He, Y., Zhang, S., Zhang, X., Baloda, M., Gurung, A.S., Xu, H., Zhang, X., Liu, G., 2011. Ultrasensitive nucleic acid biosensor based on enzyme-gold nanoparticle dual label and lateral flow strip biosensor. Biosens. Bioelectron. 26, 2018–2024.

Jans, H., Huo, Q., 2012. Gold nanoparticle-enabled biological and chemical detection and analysis. Chem. Soc. Rev. 41, 2849–2866.

Kim, K., Lee, H.B., Lee, J.W., Park, H.K., Shin, K.S., 2008. Self-assembly of poly (ethylenimine)-capped Au nanoparticles at a toluene–water interface for efficient surface-enhanced Raman scattering. Langmuir 24, 7178–7183.

Köth, A., Koetz, J., Appelhans, D., Voit, B., 2008. "Sweet" gold nanoparticles with oligosaccharide-modified poly (ethyleneimine). Colloid Polym. Sci. 286, 1317–1327.

Lien, H.L., Elliott, D.W., Sun, Y.P., Zhang, W.X., 2006. Recent progress in zero-valent iron nanoparticles for groundwater remediation. J. Environ. Eng. Manag. 16, 371–380.

Lin, Y., Li, M., Huang, L., Shen, W., Ren, Y., 2012. Involvement of heme oxygenase-1 in β-cyclodextrin-hemin complex-induced cucumber adventitious rooting process. Plant Cell Rep. 31, 1563–1572.

Liu, J., Ma, S., Zang, L., 2013. Preparation and characterization of ammonium-functionalized silica nanoparticle as a new adsorbent to remove methyl orange from aqueous solution. Appl. Surf. Sci. 265, 393–398.

Mahmoodian, H., Moradi, O., Shariatzadeha, B., Salehf, T.A., Tyagi, I., Maity, A., Gupta, V.K., 2015. Enhanced removal of methyl orange from aqueous solutions by poly HEMA-chitosan-MWCNT nano-composite. J. Mol. Liq. 202, 189–198.

Meriç, S., Kaptan, D., Ölmez, T., 2004. Color and COD removal from wastewater containing Reactive Black 5 using Fenton's oxidation process. Chemosphere 54, 435–441.

Obare, S.O., Ito, T., Balfour, M.H., Meyer, G.J., 2003. Ferrous hemin oxidation by organic halides at nanocrystalline TiO_2 interfaces. Nano Lett. 3, 1151–1153.

Pei, H., Li, F., Wan, Y., Wei, M., Liu, H., Su, Y., Chen, N., Huang, Q., Fan, C., 2012. Designed diblock oligonucleotide for the synthesis of spatially isolated and highly hybridizable functionalization of DNA-gold nanoparticle nanoconjugates. J. Am. Chem. Soc. 134, 11876–11879.

Reddy, D.A., Lee, S., Choi, J., Park, S., Ma, R., Yang, H., Kim, T.K., 2015. Green synthesis of AgI-reduced graphene oxide nanocomposites: Toward enhanced visible-light photocatalytic activity for organic dye removal. Appl. Surf. Sci. 341, 175–184.

Saha, K., Agasti, S.S., Kim, C., Li, X., Rotello, V.M., 2012. Gold nanoparticles in chemical and biological sensing. Chem. Rev. 112, 2739–2779.

Stuchinskaya, T., Moreno, M., Cook, M.J., Edwards, D.R., Russell, D.A., 2011. Targeted photodynamic therapy of breast cancer cells using antibody-phthalocyanine-gold nanoparticle conjugates. Photochem. Photobiol. Sci. 10, 822–831.

Tang, J., Kong, B., Wang, Y., Xu, M., Wang, Y., Wu, H., Zheng, G., 2013. Photoelectrochemical detection of glutathione by IrO_2-Hemin-TiO_2 nanowire arrays. Nano Lett. 13, 5350–5354.

Verma, A.K., Dash, R.R., Bhunia, P., 2012. A review on chemical coagulation/flocculation technologies for removal of colour from textile wastewaters. J. Environ. Manag. 93, 154–168.

Wang, S.T., Yan, J.C., Chen, L., 2005. Formation of gold nanoparticles and self-assembly into dimer and trimer aggregates. Mater. Lett. 59, 1383–1386.

Wang, Y., Zhu, D., Tang, L., Wang, S., Wang, Z., 2011. Highly efficient amide synthesis from alcohols and amines by virtue of a water-soluble gold/DNA catalyst. Angew. Chem. Int. Ed. 50, 8917–8921.

Xue, T., Jiang, S., Qu, Y., Su, Q., Cheng, R., Dubin, S., Chiu, C., Kaner, R., Huang, Y., Duan, X., 2012. Graphene-supported hemin as a highly active biomimetic oxidation catalyst. Angew. Chem. Int. Ed. 124, 3888–3891.

Yao, Y., Mao, Y., Huang, Q., Wang, L., Huang, Z., Lu, W., Chen, W., 2014. Enhanced decomposition of dyes by hemin-ACF with significant improvement in pH tolerance and stability. J. Hazard. Mater. 264, 323–331.

Zhang, G., Yi, L., Deng, H., Sun, P., 2014. Dyes adsorption using a synthetic carboxymethyl cellulose-acrylic acid adsorbent. J. Environ. Sci. 26, 1203–1211.

Zhong, P.S., Widjojo, N., Chung, T.S., Weber, M., Maletzko, C., 2012. Positively charged nanofiltration (NF) membranes via UV grafting on sulfonated polyphenylenesulfone (sPPSU) for effective removal of textile dyes from wastewater. J. Membr. Sci. 417, 52–60.

Zhu, H., Chen, X., Zheng, Z., Ke, X., Jaatinen, E., Zhao, J., Guo, C., Xie, T., Wang, D., 2009. Mechanism of supported gold nanoparticles as photocatalysts under ultraviolet and visible light irradiation. Chem. Commun. 48, 7524–7526.